PHYSICAL REVIEW LETTERS

Spin-Dependent Forces on Trapped Ions for Phase-Stable Quantum Gates and Entangled States of Spin and Motion

P. C. Haljan, K.-A. Brickman, L. Deslauriers, P. J. Lee, and C. Monroe

FOCUS Center and Department of Physics, University of Michigan, Ann Arbor, Michigan 48109, USA
(Received 1 November 2004; published 22 April 2005)

Favored schemes for trapped-ion quantum logic gates use bichromatic laser fields to couple internal qubit states with external motion through a "spin-dependent force." We introduce a new degree of freedom in this coupling that reduces its sensitivity to phase decoherence. We demonstrate bichromatic spin-dependent forces on a single trapped $^{111}\text{Cd}^+$ ion, and show that phase coherence of the resulting entangled states of spin and motion depends critically upon the spectral arrangement of the optical fields. This applies directly to the operation of entangling gates on multiple ions.

Trapped atomic ions have a number of desirable features that make them well suited for quantum information applications [1]. Pairs of hyperfine ground states provide an ideal host for quantum bits (qubits) that can be manipulated and entangled via optical Raman transitions [2]. Since the first proposal for entangling trapped ions [3], significant theoretical advances have relaxed the constraints on implementation to realize more robust entanglement schemes [4–7]. These schemes rely on a spin-dependent force acting on each ion where "spin" refers to the effective Pauli spin associated with the ion-qubit's two-level system. Acting on a single ion, the force can entangle the ion's spin degree of freedom with its motion; following disentanglement, the ion acquires a net geometric phase that is spin dependent [6]. When the force is applied to two ions, the geometric phase depends nonlinearly on their spins through their mutual Coulomb interaction, generating entanglement.

Optical Raman fields are a convenient way to create strong spin-dependent forces for hyperfine ion qubits [8,9]. For example, an entangling gate based on a $\hat{\sigma}_z$-dependent force has been realized with a state-dependent ac Stark shift from Raman fields [10], where $\hat{\sigma}_{x,y,z}$ are the Pauli operators. Unfortunately, such $\hat{\sigma}_z$ gates are not compatible with magnetic-field insensitive (or "clock") qubit states [2,11], and are therefore open to qubit phase decoherence from fluctuating magnetic fields. An alternative solution is the Mølmer-Sørensen (MS) gate [4,12,13], which uses a more complicated arrangement of bichromatic fields to realize a $\hat{\sigma}_\phi$-type force where $\hat{\sigma}_\phi$ is a linear combination of $\hat{\sigma}_x$ and $\hat{\sigma}_y$ operators. While the gate does work on clock states, it can have a significant phase instability due to the hyperfine coherences required to generate the spin dependence. All gates, whatever the spin dependence, are susceptible to fast phase fluctuations of the Raman fields during the course of gate evolution. However, the MS gate can also be susceptible to slow phase drifts, which cause changes in the spin dependence of the force and results in a phase instability *between* gates.

In this Letter we show how to overcome phase drifts in the MS gate, allowing clock-state benefits to be realized for ion-based qubits. Such ideas may be useful in other experimental settings since the MS scheme is a general paradigm for entanglement [14]. A bichromatic force is implemented on a single ion to demonstrate the periodic formation of states of entangled spin and motion [8]. The generation of these single-ion states is a useful test-bed for issues related to the MS gate without the added complication of two ions. We make use of the coherence of such states to demonstrate a phase-insensitive gate arrangement.

A $\hat{\sigma}_\phi$ force operates in a spin basis dressed by the Raman laser fields. It is created from a bichromatic field composed of Raman couplings to the first vibrational sidebands of the trapped ion's motion, assumed along the $\hat{z}$ axis. The red sideband coupling $|\downarrow, n+1\rangle \leftrightarrow |\uparrow, n\rangle$ and the blue coupling $|\downarrow, n\rangle \leftrightarrow |\uparrow, n+1\rangle$ create a Jaynes-Cummings and anti–Jaynes-Cummings interaction between the ion's spin and its vibrational levels $\{|n\rangle\}$ [9]. If the red and blue couplings have the same base Rabi frequencies ($\Omega_r = \Omega_b = \Omega_{sb}$ for $n = 0$) and balanced detunings ($-\delta_r = \delta_b = \delta$), then a spin-dependent, oscillating force is realized under the rotating-wave and Lamb-Dicke approximations [15] (see also Ref. [16]). The Hamiltonian in the interaction frame is

$$H_I(t) = -\frac{F_o z_o}{2}\hat{\sigma}_\phi(\hat{a}e^{\iota\delta t + \iota\phi_m} + \hat{a}^\dagger e^{-\iota\delta t - \iota\phi_m}), \quad (1)$$

where $z_o = \sqrt{\hbar/2m\omega_z}$ is the size of the harmonic oscillator ground state for an ion of mass m and center-of-mass oscillation frequency ω_z. The strength of the force is given by $F_o z_o = \hbar\Omega_{sb}$ and $\hat{a}^\dagger$ and $\hat{a}$ are the oscillator raising and lowering operators. The orientation of the force's spin dependence, $\hat{\sigma}_\phi = e^{-\iota\phi_s}\hat{\sigma}_+ + e^{\iota\phi_s}\hat{\sigma}_-$, is defined by the azimuthal angle ϕ_s where $\hat{\sigma}_\pm$ are the spin raising and lowering operators. Note $\hat{\sigma}_\phi = \hat{\sigma}_x$ for the case $\phi_s = 0$. In terms of the phases ϕ_r and ϕ_b of the red and blue sideband fields, the spin phase of the MS force in Eq. (1) is $\phi_s = (\phi_b + \phi_r)/2$ and the motional phase is $\phi_m = (\phi_b - \phi_r)/2$. The unitary evolution generated by the force is a

spin-dependent displacement $\hat{\mathcal{U}}(t) = \hat{\mathcal{D}}(\alpha(t))|\uparrow_\phi\rangle \times \langle\uparrow_\phi| + \hat{\mathcal{D}}(-\alpha(t))|\downarrow_\phi\rangle\langle\downarrow_\phi|$ where $|\downarrow_\phi\rangle$ and $|\uparrow_\phi\rangle$ are the eigenstates of $\hat{\sigma}_\phi$ [17]. $\hat{\mathcal{D}}(\alpha)$ is the displacement operator in position-momentum (z-p) phase space with $\alpha(t) = \alpha_o e^{-i\phi_m}(1 - e^{-i\delta t})$ and $\alpha_o = \Omega_{sb}/2\delta$. The corresponding position and momentum displacements are $2z_o\,\mathrm{Re}(\alpha(t))$ and $2m\omega z_o\,\mathrm{Im}(\alpha(t))$, respectively.

Instabilities in the spin and motional phases ϕ_s and ϕ_m arise from optical phase fluctuations $\delta\phi$ between the laser beams generating the Raman field at the ion (Fig. 1), or equivalently from fluctuations in the ion center-of-mass position. Slow global fluctuations in the force's motional phase are unimportant in the context of MS entangling gates, which involve only transient motional coherences associated with closed trajectories in phase space. Motional coherence between gates is therefore irrelevant. Such is not the case for spin coherences; however, bichromatic fields offer an additional degree of freedom to suppress the effect of fluctuations on ϕ_s. The two fields can be composed of copropagating or counterpropagating Raman beat waves. For the copropagating (phase-sensitive) setup in Fig. 1(a), the phase fluctuation $\delta\phi$ appears on the red and blue sideband couplings with the same sign ($\phi_r = \phi_b = \delta\phi$) and so is directly written onto the MS spin phase ($\phi_s = \delta\phi$). In the counterpropagating (phase-insensitive) case in Fig. 1(b), the phase fluctuation appears with opposite sign ($-\phi_r = \phi_b = \delta\phi$) and is thus eliminated from the spin phase ($\phi_s \equiv 0$). The phase-sensitive setup is useful for canceling common-mode fluctuations with other gate operations employing the same Raman beams while the phase-insensitive setup is useful for synchronizing with operations involving microwave fields or different Raman beam geometries. This discussion accounts for only fluctuations shared by the sideband fields as shown in Fig. 1, but independent fluctuations can also be avoided with appropriate optical design.
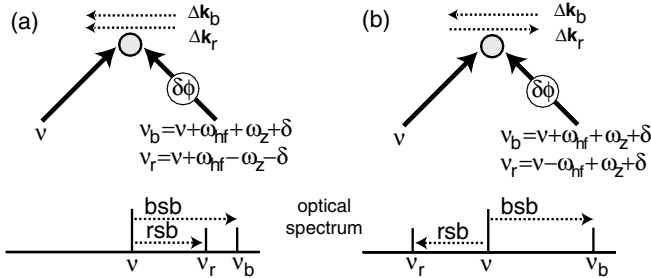

FIG. 1. Two possible Raman setups (top) to realize a bichromatic force on a hyperfine ion-qubit and corresponding optical spectrum (bottom) showing red (rsb) and blue (bsb) sideband beat notes. Two laser beams (solid lines, top) with optical carrier frequency ν generate (a) copropagating or (b) counterpropagating Raman running waves (dotted lines) at the ion with wave vectors $\Delta\mathbf{k}_{r,b}$. Symbols include optical phase fluctuation $\delta\phi$, hyperfine splitting ω_{hf}, ion-trap frequency ω_z, and force detuning δ.

Our experiment is centered around a linear ion trap [18] employing both rf and dc fields to create a harmonic confining potential, characterized by trapping frequencies $\{\omega_x, \omega_y, \omega_z\}/2\pi = \{8, 9, 3.55\}$ MHz. Single $^{111}\mathrm{Cd}^+$ ions are loaded into the trap from a neutral CdO oven source via resonant pulsed-laser photoionization. The qubit resides in the $5S_{1/2}$ ground hyperfine clock states, $|\downarrow\rangle = |F = 1, m_F = 0\rangle$ and $|\uparrow\rangle = |F = 0, m_F = 0\rangle$, separated by $\omega_{hf}/2\pi = 14.53$ GHz. Doppler cooling on the $5S_{1/2} - 5P_{3/2}$ cycling transition (wavelength 214.5 nm, linewidth $\gamma/2\pi = 58$ MHz) brings the ion to a thermal state given by $\bar{n} \approx 7$. An optional step of sideband cooling can further cool the ion to near the ground state of motion along the $\hat{z}$ axis ($\bar{n} \approx 0.05$) [18], well within the Lamb-Dicke limit. Optical pumping allows near perfect preparation of the qubit to the state $|\uparrow\rangle$. Fluorescence detection provides efficient readout of the qubit state [18].

Raman transitions are generated with a pair of laser beams in a 90° geometry with wave vector difference $\Delta\mathbf{k}$ along the $\hat{z}$ axis (Fig. 1). Coupling occurs via the $P_{3/2}$ state from which the beams are detuned by $\sim$220 GHz. A combination of laser modulation techniques is used to generate the Raman beat notes [19]. To bridge the hyperfine gap an electro-optic modulator is used to impart a microwave frequency comb onto the Raman laser, which is then split into two arms. Since the comb exists on both arms, all frequencies exist to access beat waves propagating in either direction. A pair of acousto-optic modulators (AOMs), one in each arm, generates a frequency offset between the two beams. This allows for tuning across any single motional sideband resonance associated with either wave vector direction [20]. A bichromatic Raman field is obtained by driving one AOM with two rf frequencies (Fig. 1) so that any optical phase fluctuations on the red and blue sidebands are common mode. The sideband Rabi frequencies, typically 2 kHz, are balanced *in situ* to better than 10% and the detunings δ_r and δ_b to better than 100 Hz, likely limited by ac Stark shift fluctuations induced by beam-pointing instabilities.

The action of the bichromatic force is demonstrated by applying it to a single ion, initially prepared in $|\uparrow\rangle$. This initial state can be expressed in terms of the diagonal spin basis of the bichromatic force as $\frac{1}{\sqrt{2}}(|\uparrow_x\rangle + |\downarrow_x\rangle)|0\rangle$, where without loss of generality the force is taken to be $\hat{\sigma}_x$ dependent and the initial motional state is the ground state. Application of the force generates the entangled state $\frac{1}{\sqrt{2}} \times (|\uparrow_x\rangle|\alpha\rangle + |\downarrow_x\rangle|-\alpha\rangle)$, which can be written in the measurement or $\hat{\sigma}_z$ basis as $|\uparrow\rangle(|\alpha\rangle + |-\alpha\rangle)/2 + |\downarrow\rangle(|\alpha\rangle - |-\alpha\rangle)/2$ [8,21]. Taking into account an initial thermal motional state as well as weak decoherence from motional heating [22] leads to the general expression for the probability of measuring the ion to be in state $|\downarrow\rangle$:

$$P_\downarrow^c(\tau) = \tfrac{1}{2}[1 - e^{-(1/2)\dot{\bar{n}}\tau|4\alpha_o|^2 - [\bar{n}+(1/2)]|2\alpha(\tau)|^2}]. \quad (2)$$

The initial thermal distribution is characterized by average

occupation number $\bar{n}$, the motional heating rate by $\dot{\bar{n}}$, and the duration of the force by τ.

An experiment in which the duration of the force is varied before qubit detection demonstrates the periodic entanglement in single-ion evolution (Fig. 2). A transition to $P_\downarrow^c = 1/2$ indicates when an entangled state of spin and motion is formed. At this point, the motional wave packets of the state are sufficiently far separated that spin interference is inhibited, yielding equal probability of $|\uparrow\rangle$ and $|\downarrow\rangle$. At fringe minima corresponding to $\delta\tau = 2m\pi$ with m an integer, the motional states return to their original position and overlap. The spin interference is restored, giving the initial state $|\uparrow\rangle$ such that $P_\downarrow^c \approx 0$. The periodic entanglement of spin and motional degrees of freedom continues with reasonable quality for at least two oscillations (Fig. 2).

A complementary experiment in which the force's duration is fixed but the detuning δ is varied is shown in Fig. 3. Two initial motional states have been used, a "hot" case of a Doppler cooled ion and a "cold" case of a ion cooled to near the ground state. On resonance where the force is strongest, the inferred motional wave packet separation in Fig. 3 is $\Delta z \sim 10 z_o$, a factor of 2.8 larger than the rms size of the hot ion's thermal state. The hot case has a broader envelope and narrower fringes. This occurs because the average over the initial thermal distribution quickly draws the experiment outcome towards $P_\downarrow^c = 1/2$, even for small displacements. Nevertheless, all initial states should return on themselves at the same moment (within the Lamb-Dicke approximation) giving a full revival. The overall decrease of contrast, particularly visible in the nonzero baseline, is due to spin decoherence and optical pumping induced by spontaneous emission. The detuning-dependent fringe contrast is consistent with motional decoherence which has a characteristic exponential sensitivity to the motional wave packet separation, largest near resonance ($\delta \sim 0$) [22,23].

To observe the phase sensitivity of the MS force, an interference technique is required. Ramsey interferometry combined with the formation of entangled spin-motion
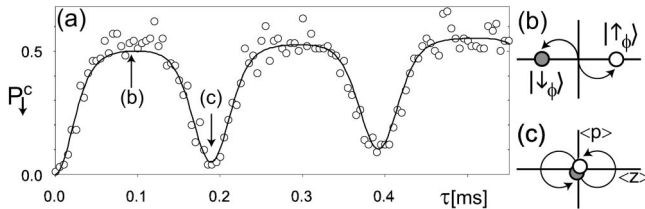
states provides a fluorescence signal that is sensitive to the orientation of the force's spin basis, characterized by phase ϕ_s. The essence of the procedure is to rotate the spin of the initial state $|\uparrow\rangle$ with a $\pi/2$ pulse into the "x-y" plane at some azimuthal angle ϕ_o. This results in the state $1/\sqrt{2}(|\uparrow\rangle + e^{\iota\phi_o}|\downarrow\rangle)$ where ϕ_o is the reference phase associated with the $\pi/2$ pulse. The force is then applied. A $3\pi/2$ analysis pulse returns the spin to the "z axis" before measurement, yielding a ϕ_s sensitive signal:

$$P_\downarrow = P_\downarrow^c(\tau)\sin^2(\phi_o - \phi_s), \qquad (3)$$

where $P_\downarrow^c(\tau)$ is given by Eq. (2). As long as the detuning and duration τ of the force are chosen to generate a significant displacement ($\alpha \gg 1$), the signal is approximately $\frac{1}{2}\sin^2(\phi_o - \phi_s)$. If the initial $\pi/2$ pulse rotates the ion's spin into a state in which the force is diagonal ($\phi_o = \phi_s + m\pi$ with m an integer), a displacement occurs but no entangled spin-motion state is formed. Thus following the analysis pulse, the ion's spin returns to its initial state $|\uparrow\rangle$ such that $P_\downarrow = 0$. On the other hand, if the rotated initial state deviates from this special condition ($\phi_o \neq \phi_s + m\pi$), then the state is a superposition of the force's spin basis and an entangled spin-motion state is formed. This is revealed by a net fluorescence signal on analysis.

An optical Raman carrier transition (90° geometry) is used for the interferometry pulses. The actual pulse sequence is a photon-echo scheme where the $3\pi/2$ analysis
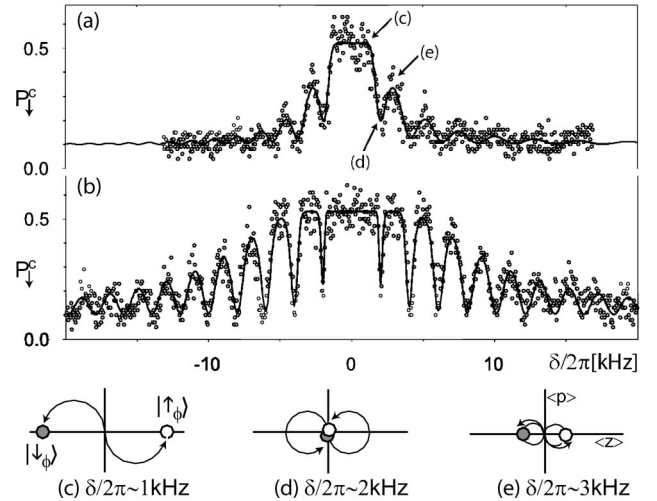
FIG. 3. Probability $P_\downarrow^c$ plotted vs detuning δ of the bichromatic force for (a) a ground-state cooled and (b) a Doppler cooled ion, initially prepared in $|\uparrow\rangle$. The force is applied for 500 μs. Data are run-time averaged with 100 shots/point. Solid lines show fits to Eq. (2) modified to include overall peak and contrast factors (for spontaneous emission) and a detuning drift across the data. An initial fit to (a) assuming $\bar{n} = 0.05$ gives $\Omega_{sb}/2\pi = 1.6$ kHz and $\dot{\bar{n}} = 0.4$ ms^{-1}. A subsequent fit to (b) assuming $\Omega_{sb}/2\pi = 1.6$ kHz gives $\bar{n} = 6$ and $\dot{\bar{n}} = 0.5$ ms^{-1}. The values of $\dot{\bar{n}}$ are reasonably consistent with the directly measured heating rate 0.2 ms^{-1} [18]. Phase space sketches (c)–(e) indicate ion evolution at detunings referenced in (a).
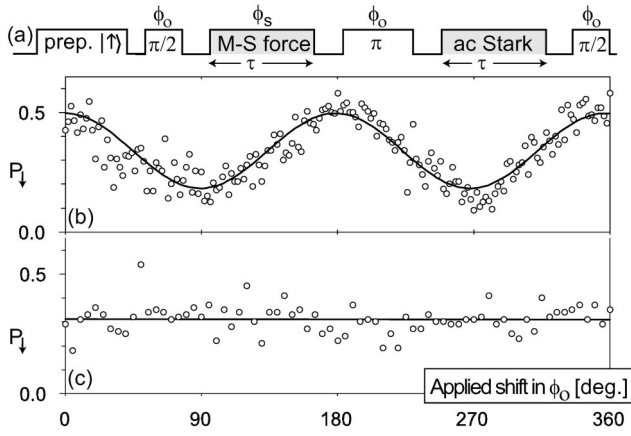
FIG. 2. Single-ion evolution due to a spin-dependent bichromatic force. (a) Probability $P_\downarrow^c$ of measuring state $|\downarrow\rangle$ plotted vs force duration τ. Ion is initially Doppler cooled, and data run-time averaged (100 shots/point). Solid line is a fit to Eq. (2) modified to include a linear change in peak and contrast (from spontaneous emission) and a detuning drift across the data. The fit gives $\delta/2\pi = -5.5$ kHz and constrains $\bar{n}\Omega_{sb}^2$ to $\bar{n} = 5$–10 for $\Omega_{sb}/2\pi = 2.2$–1.6 kHz. (b),(c) Phase space sketches of the ion motion at points indicated in (a).

FIG. 4.   (a) Interferometric photon-echo sequence to test optical phase sensitivity of the MS force. Phase ϕ_o and duration of spin-rotation pulses (unshaded) indicated. The MS pulse (with spin phase ϕ_s) and pulse for ac Stark shift compensation are shown shaded. (b),(c) Probability $P_\downarrow$ plotted vs applied shift in ϕ_o where (b) and (c) correspond to setups in Figs. 1(a) and 1(b) respectively. Data are run-time averaged with 100 shots/point requiring $\sim$200 ms/point. Parameters include $\pi/2$ pulse time of 13 μs, $\Omega_{sb}/2\pi \approx 2$ kHz, $\delta/2\pi \approx 5$ kHz, $\tau = 90$ μs, and $\bar{n} \approx 7$. Solid lines are a sinusoidal fit (b) and a linear fit (c).

pulse is divided into a π and a $\pi/2$ pulse [Fig. 4(a)]. This provides a convenient way to cancel the effect of Stark shifts ($\sim$ 20 kHz) from the optical carrier pulses as well as from the MS force itself. The Stark-induced phase from the MS pulse is canceled by introducing a bichromatic pulse, far detuned from the motional resonance, into the second echo zone [Fig. 4(a)].

The carrier pulses which act as a phase reference are subject to the same optical phase drifts as the sidebands creating the bichromatic force. Therefore the interferometric signal $P_\downarrow$ is expected to be stable for the phase-sensitive Raman setup [Fig. 1(a)] where fluctuations in the force's spin phase ϕ_s are common to the reference phase ϕ_o. A scan of the reference phase [Fig. 4(b)] shows interference fringes with nearly full contrast (maximum being 1/2). This remains the case even with a piezoelectric transducer slowly (1 Hz) modulating one Raman arm by an optical wavelength. Washout of the interferometric signal should occur when the MS force is generated with the phase-insensitive setup [Fig. 1(b)]. In this case, the force's spin dependence, now decoupled from instabilities, is no longer correlated with optical phase fluctuations on the carrier pulses. This configuration did not require the addition of Raman path-length modulation to spoil the fringe contrast as inherent phase drifts on the optical table were a sufficient noise source over the 200 ms experiment averaging time.

A spin-dependent force for clock-state qubits has been demonstrated that can be combined with other operations in a way that is insensitive to slow optical phase fluctuations and drifts in the ion center-of-mass position. This opens the way to phase-stable algorithms as follows: Single qubit rotations can be implemented with a copropagating Raman transition or microwaves. The entangling gate may be realized directly with a $\hat{\sigma}_\phi$-dependent force based on the phase-insensitive setup. Alternatively, the phase-sensitive setup can be used in a composite sequence as in Fig. 4(a) to construct a $\hat{\sigma}_z$ gate where the carrier pulses act as a $\hat{\sigma}_z \leftrightarrow \hat{\sigma}_\phi$ transformation. This arrangement can also suppress phase noise due to slow drifts in the relative position of two ions.

[1] D. J. Wineland et al., J. Res. Natl. Inst. Stand. Technol. **103**, 259 (1998).
[2] B. B. Blinov et al., Quant. Info. Proc. **3**, 45 (2004).
[3] J. I. Cirac and P. Zoller, Phys. Rev. Lett. **74**, 4091 (1995).
[4] K. Mølmer and A. Sørensen, Phys. Rev. Lett. **82**, 1835 (1999).
[5] E. Solano, R. L. de Matos Filho, and N. Zagury, Phys. Rev. A **59**, R2539 (1999).
[6] G. J. Milburn, S. Schneider, and D. F. V. James, Fortschr. Phys. **48**, 801 (2000).
[7] J. J. Garcia-Ripoll, P. Zoller, and J. I. Cirac, Phys. Rev. Lett. **91**, 157901 (2003).
[8] C. Monroe et al., Science **272**, 1131 (1996).
[9] D. Leibfried et al., Rev. Mod. Phys. **75**, 281 (2003).
[10] D. Leibfried et al., Nature (London) **422**, 412 (2003).
[11] C. Langer and D. J. Wineland (private communication).
[12] C. A. Sackett et al., Nature (London) **404**, 256 (2000).
[13] A. Sørensen and K. Mølmer, Phys. Rev. A **62**, 022311 (2000).
[14] X. Wang, A. Sorensen, and K. Molmer, Phys. Rev. Lett. **86**, 3907 (2001); K. Helmerson and L. You, Phys. Rev. Lett. **87**, 170402 (2001); S. Osnaghi et al., Phys. Rev. Lett. **87**, 037902 (2001).
[15] S. Wallentowitz and W. Vogel, Phys. Rev. Lett. **75**, 2932 (1995); S.-B. Zheng, Phys. Rev. A **58**, 761 (1998); H. Moya-Cessa, S. Wallentowitz, and W. Vogel, Phys. Rev. A **59**, 2920 (1999); E. Solano et al., Phys. Rev. Lett. **87**, 060402 (2001).
[16] E. Solano, G. S. Agarwal, and H. Walther, Phys. Rev. Lett. **90**, 027903 (2003).
[17] A global displacement-induced phase omitted from $\hat{U}(t)$.
[18] L. Deslauriers et al., Phys. Rev. A **70**, 043408 (2004).
[19] P. J. Lee et al., Opt. Lett. **28**, 1582 (2003).
[20] The EOM is tuned so all transitions are well resolved.
[21] R. L. de Matos Filho and W. Vogel, Phys. Rev. Lett. **76**, 608 (1996).
[22] Q. A. Turchette et al., Phys. Rev. A **61**, 063418 (2000).
[23] D. F. Walls and G. J. Milburn, Phys. Rev. A **31**, 2403 (1985).